

## Cumulative Damage Theory in Fatigue of Graphite/Epoxy [ $\pm 45$ ]<sub>s</sub> Composites

Deuk Man An<sup>†</sup>

**ABSTRACT:** The phenomenological evolution laws of damage can be defined either based on residual life or residual strength. The failure of a specimen can be defined immediately after or before fracture. The former is called in this paper by “failure defined by approach I” and the latter “failure defined by approach II.” Usually at failure there is a discontinuity of loading variables and, because of this, damage at failure is discontinuous. Therefore the values of damage at failure by two different approaches are not the same. Based on this idea the sequence effects of the phenomenological evolution law of damage given by  $dD/dN = g(D)f(\Phi)$  were studied. Thin-walled graphite/epoxy tubes consisting of four of [ $\pm 45$ ]<sub>s</sub> laminates were used for the experimental study of sequence effects and the effects of mean stress on fatigue life. It was found that the sequence effects in two step uniaxial fatigue for [ $\pm 45$ ]<sub>s</sub> graphite/epoxy tubular specimen showed that a high-low block loading sequence was less damaging than a low-high one.

**Key Words:** Cumulative damage, Graphite/epoxy composite, Residual life, Residual strength, Fatigue damage, Phenomenological laws

### 1. INTRODUCTION AND HISTORICAL REVIEW

When a structural part is subjected to static and/or time varying loading, the prediction of remaining life is an important area of mechanical design. This problem is known in the literature as the cumulative damage problem [1]. The progress of damage in a structural part can be thought of in many different ways. For a microscopic view, we can take the initiation and growth of voids and micro cracks or the increase of the dislocation density as indicators of the evolution of the damage process [2]. From a macroscopic view point, growth of macro cracks or changes of specimen geometries can be candidates for the identification of the damage.

Also, damage can be expressed as changes in mechanical properties of a material, i.e. Young's modulus, shear modulus, Poisson's ratio, yield strength, ultimate tensile strength, etc..

In the case of isotropic damage, Lemaitre [3] selected for the measurement of damage,  $D$ , the increase of effective Cauchy stress tensor in a given loading condition:

$$\sigma'_{ij} = \frac{\sigma_{ij}}{1-D} \quad (1.1)$$

where  $\sigma_{ij}$  with and without a prime denote the Cauchy stress tensor in the damaged state and undamaged state, respectively. In equation (1.1), the undamaged state is  $D = 0$ , and  $D = 1$  corresponds to the failure of the element.

If we denote ultimate tensile strength at the virgin state and at the damaged state as  $\sigma_{UTS}$ ,  $\sigma'_{UTS}$ , respectively, then damage can be defined as

$$D = 1 - \frac{\sigma'_{UTS}}{\sigma_{UTS}} \quad (1.2)$$

If the loading condition is fatigue, we might assume that during each cycle a certain amount of life of the specimen is expended and so damage can be linked to the consumption of life. Based on this idea, Palmgren [4] and later Miner [5] determined the remaining life under variable amplitude loading. Those studies usually called the Palmgren-Miner cumulative damage theory, or Miner's rule. A failure in a multistage loading or block loading (a sequence of loading segments with constant amplitude) is defined by

$$\sum_{i=1}^m \frac{n_i}{N_i} = 1 \quad (1.3)$$

where  $m$  is the number of loading segments and  $n_i$  the number of applied cycles at stress amplitude  $\sigma_i$  (segment  $i$ ) and  $N_i$  denotes the fatigue life related to  $\sigma_i$ . By (1.3) the number of cycles at the final stage,  $n_m$ , is

$$n_m = N_m \left( 1 - \sum_{i=1}^{m-1} \frac{n_i}{N_i} \right) \quad (1.4)$$

But equation (1.3) has drawback. The order in which the various stress levels are applied does not have any influence upon fatigue. For many cases in metal fatigue a high-low block loading sequence is more damaging than a low-high one [1,6]. In laminated composites the trends appear to be opposite to those in metals [7]. To reproduce the observed sequence effects in fatigue, Hashin and Rotem [8], and Hashin [9] introduced the damage curves which are defined by the remaining number of cycles-to-failure at a given equivalent cyclic loading. For a two-stage loading there is opposite behavior in sequence effects in their theory whether damage curves pass thorough the static ultimate strength or through the endurance limit. Fig. 1 shows two different sets of damage lines. Before Hashin and Rotem [8], Hashin [9], Subramanian [10] considered the sequence effects using equivalent damage curves which all pass through the knee point of the S-N curve. It corresponds to the endurance limit in Hashin and Rotem [8], and Hashin [9].

In composite materials, Broutam and Sahu [11] gave a modified Miner's rule based on their experimental results. Their definition of damage is given by equation (1.2).

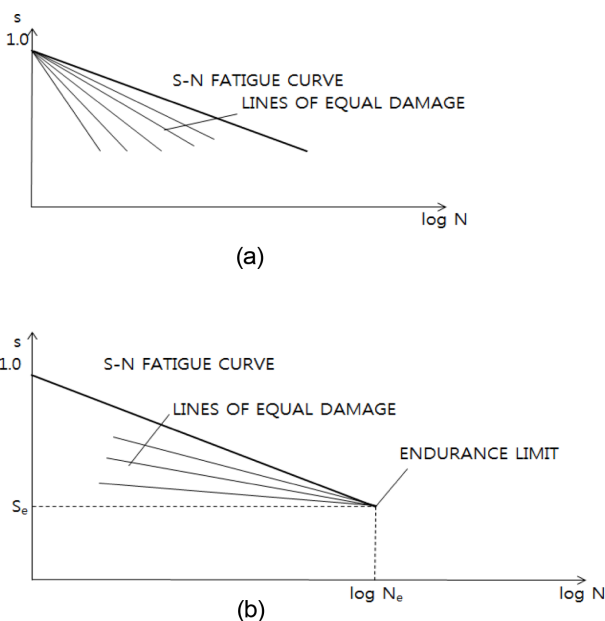


**Fig. 1.** (a) Damage lines through static ultimate strength, (b) Damage lines through endurance limit

In terms of statistics, Bogdanoff attacked the problem of cumulative damage using the Markoff process [12]. Hashin [13] provided a statistical cumulative damage theory of fatigue based on his deterministic cumulative damage theory [9] by making the assumption of normal distribution of experimental data. Yang and Jones [14] and Chou [15] assumed a two-parameter Weibull distribution of ultimate tensile strength for the prediction of fatigue life. Bengtsson and Rychik [16] and Rychlik and Gupta [17] studied fatigue damage by Gaussian loads.

All the proposed phenomenological theories of cumulative damage can be classified in two groups depending on the definition used. In the first group the damage is related to the changes in mechanical properties of a material. In the second group damage is measured by the remaining life under a certain reference loading. The former will be called the definition of damage by residual strength; the latter will be called the definition of damage by residual life.

The concept of discontinuity of damage at the failure will be introduced. A concept similar to this one was used by Bui *et al.* [18].

## 2. THE CONCEPT OF THE DISCONTINUITY OF DAMAGE AT FAILURE

To introduce the idea of the discontinuity of damage at failure, a constant stress creep test with applied stress level  $\sigma_{CP}$  is taken as an example. As shown in Fig. 2, during this creep

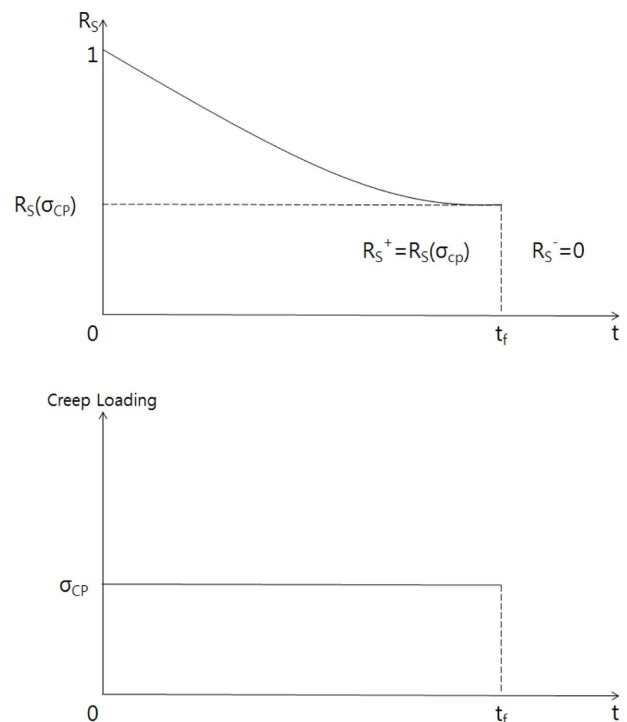


**Fig. 2.** A schematic diagram of decrease of residual strength under constant creep loading ( $\sigma_{CP}$ )

loading, residual strength  $R_s$  is supposed to decrease from one to the residual strength  $R_s(\sigma_{CP})$  which is the value corresponding to the stress level  $\sigma_{CP}$ . Immediately after the specimen is broken, no external load can be sustained by this specimen and therefore the corresponding residual strength is zero. By considering residual strength immediately before and after the failure, we can conceive a discontinuity of residual strength at the failure time  $t_f$ . Adopting usual designations in describing discontinuity of real functions, we can express the residual strength immediately before and after time  $t_f$  as follows:

$$R_s^- = R_s(\sigma_{CP}) \tag{2.1a}$$

$$R_s^+ = 0 \tag{2.1b}$$

where superscripts “-” and “+” denotes the values of the residual strength as the failure time  $t_f$  is approached from the left and right, respectively. Fig. 2 shows the discontinuity of residual strength at  $t_f$ . We can introduce damage,  $D$ , by one-to-one mapping with the residual strength,  $R_s$ . For this one-to-one mapping we have a damage discontinuity at  $t_f$ .

For another example of damage discontinuity, let us consider a single-edge notched specimen with constant stress amplitude zero-to- $\sigma$  fatigue loading. Fig. 3 shows a schematic. Here we can define the damage,  $D_1$  in the form

$$D_1 = \frac{a}{2b} \tag{2.2}$$

where  $a$  is the current crack length and  $2b$  the width of the

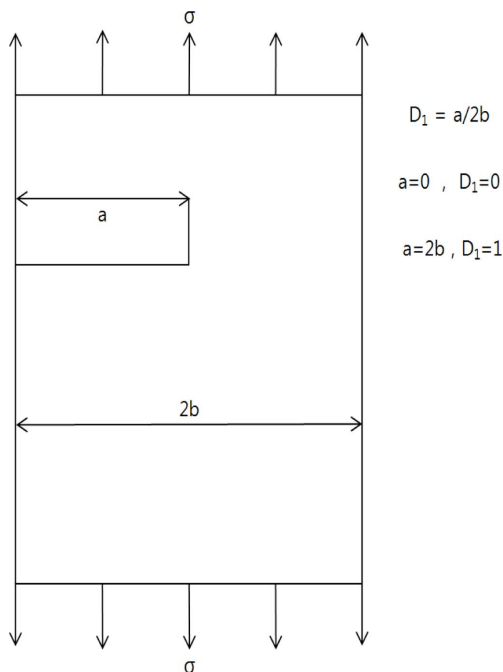


Fig. 3. Example of damage definition for a single-edge-notched specimen

specimen. From the above definition we have a one-to-one relationship between crack length  $a$  and the damage  $D_1$  and in particular we have

$$a = 0 \leftrightarrow D_1 = 0$$

$$a = 2b \leftrightarrow D_1 = 1 \tag{2.3}$$

The laws of linear elastic fracture mechanics indicate that the specimen has the critical crack length  $a$  for a given nominal stress  $\sigma$ . If the crack length exceeds  $a$ , there occurs catastrophic failure of the specimen so we can express a discontinuity of damage at failure.

$$D_{1f}^- = \frac{a_c}{2b} \tag{2.4a}$$

$$D_{1f}^+ = 1 \tag{2.4b}$$

where  $D_{1f}$  denotes the damage at the failure.

In general loading conditions there always exist abrupt changes (discontinuities) of forcing variables at failure time  $t_f$ . Actually forcing variables drop to zero; so, if damage,  $D$ , depends on forcing variables continuously, we have always a discontinuity of damage at failure. Because of discontinuity of damage at failure, we have two choices for the identification of damage at the failure,  $D_f$ : one is defined at the damage immediately after failure; and the other is defined at the damage immediately before failure. We will call the former the damage at the failure defined by approach I; the latter will be called the damage at the failure defined by approach II. Since after the specimen is failed no load (or forcing variables) can be carried, the damage at the failure by approach I ( $D_{1f}^+$  or  $D_f^+$ ) is always a constant value (one or infinity) which is the value corresponding to the residual strength zero. However, the damage at the failure by approach II ( $D_{1f}^-$  or  $D_f^-$ ) is dependent on forcing variables immediately before failure time  $t_f$  so it is gen-

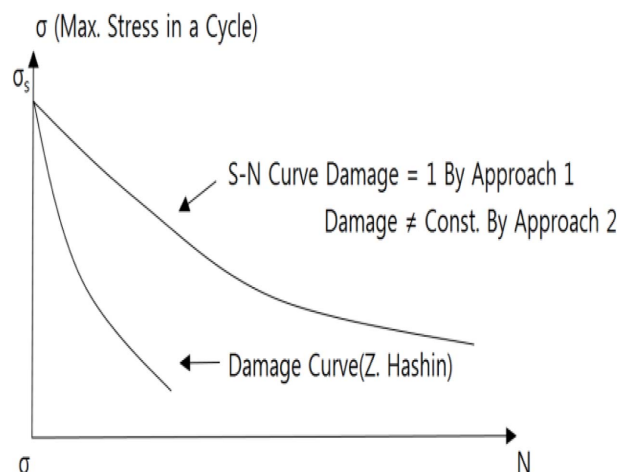


Fig. 4. S-N fatigue curve

erally not constant. For an example, the usual S-N curve can have two interpretations. Using approach I the S-N curve corresponds to the same damage,  $D_{1f}^+ = 1$  or  $D_{1f}^+ = \infty$ ; but by approach II the damage along the S-N curve will be different because of the difference of forcing variables.

Fig. 4 shows a schematic. Based on this concept we can classify existing cumulative damage theories. Miner [5], Hashin and Rotem [8], Hashin [9], Subramanyan [10], Bui-Quoc [19], etc. used the definition of damage at failure by approach I. Broutman and Sahu [11], Yang and Jones [14], etc. used the definition of damage at failure by approach II.

### 3. SEQUENCE EFFECTS IN FATIGUE

Based on previous discussions of the discontinuity of damage at failure and definitions of failure by approach I and approach II, we now examine the sequence effects (in fatigue) for the particular differential evolution law of damage employed by Yang and Jones [14]. This equation is given by

$$\frac{dD}{d\eta} = g(D)f\left(\Phi, \frac{d\Phi}{d\eta}\right) \quad (3.1)$$

where

$\Phi$  = dimensionless forcing variable

$\eta$  = dimensionless time.

If we do not consider the effect of rate of the forcing variable, we can rewrite equation (3.1) as

$$\frac{dD}{dN} = g(D)f(\tilde{\Phi}) \quad (3.2)$$

where  $N$  is the number of cycles and  $\tilde{\Phi}$  is the appropriate forcing variable. For the stress control fatigue we can identify  $\tilde{\Phi}$  as the absolute maximum stress of the generalized amplitude during a cycle. If we do not consider the process of the recovery of damage, the functions  $g(D)$  and  $f(\tilde{\Phi})$  can be only zero when its argument is zero since it is required that no damage accumulates in the absence of external loading. If we identify the damage  $D$  as the crack length  $a$ , equation (3.2) is of the same form as used by Paris and Erdogan [20] in the study of fatigue crack growth,

$$\frac{da}{dN} = A(\Delta K_I)^n \quad (3.3)$$

where  $A$  and  $n$  are constants, and  $\Delta K_I$  is the difference between the maximum and the minimum stress intensity factors for Mode I in a cycle.

Let us define Miner's coefficient in two-state stress-controlled loading as shown in Fig. 5 as:

$$M = \frac{n_1}{N_1} + \frac{n_2}{N_2} \quad (3.4)$$

where  $n_i$ ,  $N_i$  ( $i = 1, 2$ ) are the number of cycles and the fatigue life at the stress level  $\sigma_i$ , respectively. Let us introduce damage,

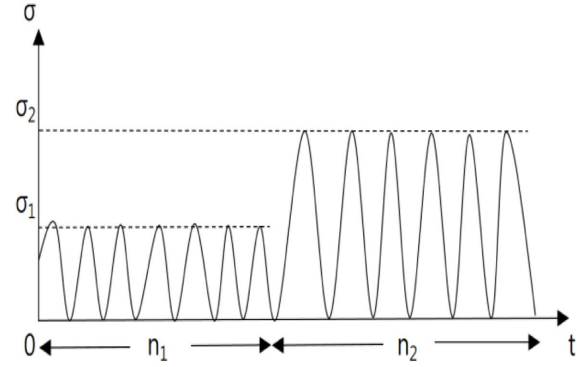


Fig. 5. Two-state stress controlled loading

$D$ , in the form

$$D = \frac{1}{R_S} - 1$$

Then we can change  $D$  to  $R_S$  in equation (3.2) as

$$-\frac{dR_S}{dN} = \tilde{g}(R_S)f(\tilde{\Phi}) \quad (3.5)$$

where

$$\tilde{g}(R_S) = f(D(R_S)).$$

The residual strength at the failure by using approach II is

$$R_S^- = R_S(\sigma)$$

and by approach I we have

$$R_S^+ = 0.$$

First we calculate Miner's coefficient using approach I. Knowing the residual strength at the failure is zero and integration from  $N = 0$  to  $n_1 + n_2$ , equation (3.5) becomes

$$\int_1^0 -\frac{dR_S}{\tilde{g}(R_S)} = \int_0^{n_1+n_2} f(\tilde{\Phi}) dN \quad (3.6)$$

but during each of  $n_1$  and  $n_2$  cycles there is no change in forcing variable  $\tilde{\Phi}$ . For this reason equation (3.6) can be written as

$$\int_0^1 \frac{dR_S}{\tilde{g}(R_S)} = n_1 f(\tilde{\Phi}_1) + n_2 f(\tilde{\Phi}_2) \quad (3.7)$$

where  $\tilde{\Phi}_i$  ( $i = 1, 2$ ) are appropriate forcing variables in each block of loading. By equation (3.7) the fatigue lives  $N_1$  and  $N_2$  by approach I are

$$N_1 = \frac{1}{f(\tilde{\Phi}_1)} \int_0^1 \frac{dR_S}{g(R_S)} \quad (3.8)$$

and

$$N_2 = \frac{1}{f(\tilde{\Phi}_2)} \int_0^1 \frac{dR_S}{\tilde{g}(R_S)} \quad (3.9)$$

From equation (3.7) the remaining life  $n_2$  after  $n_1$  cycles under the first block loading is

$$n_2 = \frac{1}{f(\tilde{\Phi}_2)} \int_0^1 \frac{dR_S}{\tilde{g}(R_S)} - n_1 \frac{f(\tilde{\Phi}_1)}{f(\tilde{\Phi}_2)} \quad (3.10)$$

Using equation (3.8) and (3.9),  $n_2/N_2$  becomes

$$\begin{aligned} \frac{n_2}{N_2} &= \frac{f(\tilde{\Phi}_2)}{f(\tilde{\Phi}_2)} \cdot \frac{1}{\int_0^1 \frac{dR_S}{\tilde{g}(R_S)}} \int_0^1 \frac{dR_S}{\tilde{g}(R_S)} - \frac{n_1 f(\tilde{\Phi}_1)}{N_2 f(\tilde{\Phi}_2)} \\ &= 1 - \frac{n_1 N_2}{N_2 N_1} = 1 - \frac{n_1}{N_1} \end{aligned}$$

Then the Miner's coefficient (3.4) is

$$M = \frac{n_1}{N_1} + \frac{n_2}{N_2} = 1$$

Therefore there is no sequence effect in the damage evolution law in the form of equation (3.2) and the definition of failure by approach I. However, by the definition of failure by approach II the lifetime  $N_1$  and  $N_2$  can be expressed as follows

$$N_1 = \frac{1}{f(\tilde{\Phi}_1)} \int_{R_S(\sigma_1)}^1 \frac{dR_S}{\tilde{g}(R_S)} \quad (3.11)$$

and

$$N_2 = \frac{1}{f(\tilde{\Phi}_2)} \int_{R_S(\sigma_2)}^1 \frac{dR_S}{\tilde{g}(R_S)} \quad (3.12)$$

where  $R_S(\sigma_1)$  and  $R_S(\sigma_2)$  are the residual strength corresponding to the stress levels  $\sigma_1$  and  $\sigma_2$ , respectively. In this case, Miner's coefficient is

$$M = 1 + \frac{n_1}{N_2} \left( 1 - \frac{\int_{R_S(\sigma_1)}^1 \frac{dR_S}{\tilde{g}(R_S)}}{\int_{R_S(\sigma_2)}^1 \frac{dR_S}{\tilde{g}(R_S)}} \right) \quad (3.13)$$

If  $\sigma_1 > \sigma_2$ , then  $R_S(\sigma_1) > R_S(\sigma_2)$ . With the assumption of positiveness of the function  $\tilde{g}(R_S)$  we have

$$\int_{R_S(\sigma_1)}^1 \frac{dR_S}{\tilde{g}(R_S)} < \int_{R_S(\sigma_2)}^1 \frac{dR_S}{\tilde{g}(R_S)} \quad (3.14)$$

Therefore Miner's coefficient is greater than one for  $\sigma_1 > \sigma_2$ . And, if we apply the low amplitude loading block first ( $\sigma_1 > \sigma_2$ ), the Miner's coefficient is less than one.

Ostergren and Krempl [21] showed sequence independence of the damage evolution equation (3.2), using approach I, and Yang and Jones [14] showed sequence dependence using approach II for the equation (3.2). However, none of them had the concept of the discontinuity of damage at the failure.

## 4. EXPERIMENTAL INVESTIGATION AND RESULTS

### 4.1 Specimens and Material Used

The configuration of specimens used in this study is shown in Fig. 6. All tubes are made of Graphite/Epoxy prepreg with stacking sequence  $[\pm 45]_s$ . Detailed descriptions of the techniques for specimen manufacturing can be found in [22] and [23].

Materials used in this study include Fiberite hy-E 1048 A1E, 3048 A1k, and 1248 A1F unidirectional prepreg tapes. According to the specifications of these Fiberite prepreps, the only difference between those different unidirectional prepreps is the volume percentage of the resin content. It varies from 39% for Hy-E 1248 A1F to 41% for Hy-E 1048 A1E. Mechanical properties of Hy-E 3048 A1K unidirectional composites are listed in Table 1.

For convenience in designating specimens, Hy-E 1048 A1E, 3048 A1K and 1248 A1F are denoted as A, B and C, respec-

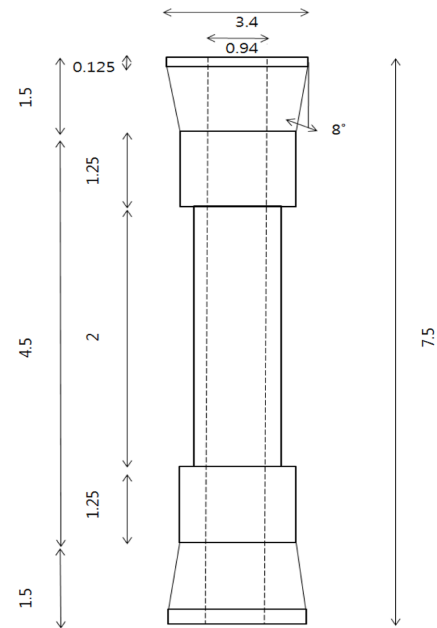


Fig. 6. Thin-walled tubular specimen

Table 1. Mechanical Properties of Fiberite Hy-E 3048 A1K

|                       |                         |
|-----------------------|-------------------------|
| $\sigma_{1f}$         | 1.345 GPa ( 195 ksi )   |
| $\sigma_{2f}$         | 30 MPa ( 4.35 ksi )     |
| $E_1$                 | 133.8 GPa ( 19,400 ksi) |
| $E_2$                 | 8.464 GPa ( 1,230 ksi)  |
| $G_{12}$              | 4.997 GPa ( 725 ksi)    |
| $\nu_{12}$            | 0.294                   |
| $\nu_{21}$            | 0.024                   |
| $t_{ply}$ (thickness) | 0.14732 (mm)            |

tively. The following convention is adopted for the identification of specimen:

B                    I                    I  
material used    batch number    specimen number

If specimens are of the same batch, they are cured at the same time.

#### 4.2a Overview and Purpose of Tests

Static tension was performed for the determination of ultimate tensile strength.

Pure axial fatigue tests with different R-ratios were performed for the axial fatigue properties and for the study of the effect of R-ratio.

Two-block loading fatigue tests were done for the study of sequence effects. After cyclic loading, the residual strength was measured. All fatigue tests were done at a frequency of 5 Hz.

Because of thicker shoulders of the specimen (see Fig. 6) the failure location was in the gage section. In all tests failure was defined as separation of the specimens.

#### 4.2b Testing Equipment

All tests were carried out in an MTS axial-torsional closed-loop servo-hydraulic testing system.

For the measurement of strain in the study of sequence effects an Instron Bialxial Extensometer model A444-8 was used; and for rest of the experiments uniaxial strain was measured by an MTS extensometer model 632.11B-20.

#### 4.3 Static Tests

For the determination of ultimate tensile strength,  $\sigma_u$ , and shear strength,  $\tau_u$ , load control was used. A sine wave of 0.01 Hz with maximum load of 2k1b in axial tests and a maximum torque of 2k1b-in. in torsional tests are employed, respectively. Experimental results are listed in Table 2.

**Table 2.** Ultimate Tensile Strength and Shear Strength of graphite/epoxy [ $\pm 45$ ]<sub>s</sub> Tubes

| Specimen Number | $\sigma_{UTS}$ (MPa) |
|-----------------|----------------------|
| B-1-6           | -131.7               |
| B-2-4           | 134.9                |
| B-2-5           | 144.6                |
| B-2-19          | 148.0                |
| B-3-10          | 144.6                |
| B-4-5           | 144.6                |
| B-5-1           | 145.0                |
| B-6-4           | 125.0                |
| B-6-7           | 117.0                |
| B-6-5           | 145.0                |

#### 4.4 Pure Axial Fatigue

Pure axial fatigue tests were done with different R-ratios (or simply R). R-ratio is defined as

$$R\text{-ratio} = \frac{\sigma_{\min}}{\sigma_{\max}} \quad (4.1)$$

where  $\sigma_{\min}$  and  $\sigma_{\max}$  are the (algebraically) minimum stress and maximum stress during a cycle, respectively. In this definition, when  $\sigma_{\max}$  becomes zero, equation (4.1) is undefined. For this reason, the inverse of equation (4.1) is taken in the case of  $\sigma_{\max} = 0$  and denoted as

$$R\text{-ratio (or } R) = 0 \quad (4.2)$$

When  $\sigma_{\min} = 0$

$$R = 0_- \quad (4.3)$$

Except for two cases, R-ratio is defined as in equation (4.1).

**Table 3.** Pure Axial Fatigue Data with Different R-ratios

| Specimen Number | $\sigma_a$ (MPa) | R  | $N_f$ (Cycles)      |
|-----------------|------------------|----|---------------------|
| B-2-6           | 73.2             | -1 | 2                   |
| B-2-1           | 73.2             | -1 | 267                 |
| B-2-7           | 57.87            | -1 | 1,500               |
| B-3-9           | 57.87            | -1 | 1,000               |
| B-2-9           | 57.87            | -1 | 1,000               |
| B-2-8           | 38.53            | -1 | 317,910             |
| B-2-10          | 38.53            | -1 | 462,910             |
| B-2-13          | 38.53            | 0- | 75,000              |
| B-2-14          | 57.87            | 0- | 400                 |
| B-2-15          | 57.87            | 0- | 610                 |
| B-2-12          | 38.53            | 0  | 23,910              |
| B-2-11          | 28.93            | 0  | 143,910             |
| B-5-6           | 59.23            | 0  | 200                 |
| B-5-5           | 54.56            | 0  | 5,400               |
| B-5-8           | 51.44            | 0  | 4,400               |
| B-5-7           | 51.44            | 0  | 5,700               |
| B-5-4           | 51.44            | 0  | 4,000               |
| B-7-7           | 54.56            | 0  | 3,000               |
| B-5-3           | 46.76            | 0  | 13,000              |
| B-8-7           | 46.76            | 0  | 9,000               |
| B-8-10          | 46.76            | 0  | 4,000               |
| B-5-2           | 43.65            | 0  | 53,000              |
| B-7-5           | 35.85            | 0  | 56,000              |
| B-1-2           | 31.07            | 0  | >10 <sup>6</sup> *) |

\*) Specimen runs out.

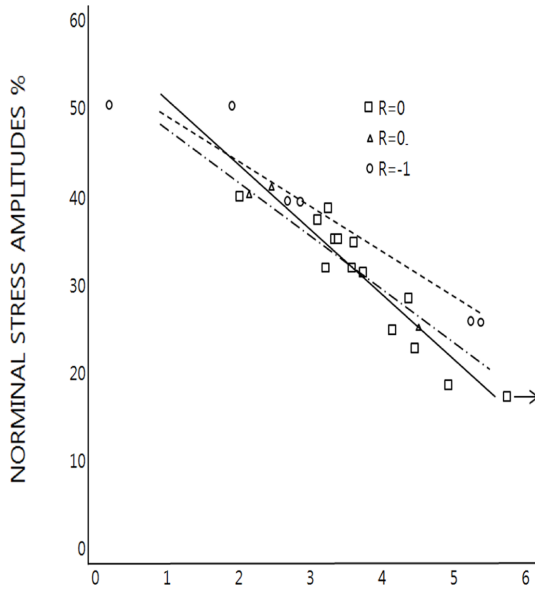


**Fig. 7.** The influence of mean stress on the axial fatigue behaviour of  $[\pm 45]_s$  graphite/Epoxy tubes

All the fatigue tests were done at 5 Hz in a sinusoidal load variation with R-ratios 0 and  $-1$ . R-ratio equals to  $-1$  corresponds to the completely reversed loading. Table 3 and Fig. 7 show the results. In Table 3  $\sigma_a$  is defined as

$$\sigma_a = \frac{\sigma_{\max} - \sigma_{\min}}{2} \quad (4.4)$$

#### 4.5 Two-step Loading Fatigue

Two-block loading fatigue in the axial direction was applied to the specimen for the study of the sequence effects.  $R = 0$  was employed with a frequency of 5 Hz. Fig. 5 shows a schematic diagram for a two-block loading fatigue. For each specimen the stiffness in the axial direction was measured at the beginning of the test and after the first block loading. For the measurement of the stiffness in the axial direction, the Instron Biaxial Extensometer model A444-8 was used. All the results are listed in Table 4.

#### 4.6 Residual Strength Tests

Residual strength is defined in the form

$$R_s = \frac{R'_{UTS}}{R_{UTS}} \quad (4.5)$$

where  $R_{UTS}$  and  $R'_{UTS}$  are ultimate tensile strength at the virgin state and at the damaged state, respectively. The following tests were performed at  $R = 0$  and at a frequency of 5 Hz. At first the drop of the residual strength with cycles was determined with the results given in Table 5. The circles in the figure 8 indicate the residual strength after a fatigue test with  $\sigma_a = 46.8$  MPa which was terminated at the indicated number of cycles. Subsequently a tensile test was performed and the ultimate tensile strength was plotted on the ordinate.

**Table 4.** Two-step Fatigue Results for graphite/epoxy  $[\pm 45]_s$ ,  $R = 0$  at 5 Hz

| S.N     | $\sigma_{a1}^*$ (MPa) | $\sigma_{a2}^*$ (MPa) | $E_0^{**}$ (GPa) | $E_1^{**}$ (GPa) | $n_1$   | $n_2$   |
|---------|-----------------------|-----------------------|------------------|------------------|---------|---------|
| C-10-9  | 39.0                  | 35.9                  | 11.62            | 10.29            | 30,000  | 54,273  |
| C-10-3  | 35.9                  | 39.0                  | 11.72            | 10.60            | 54,273  | 19,599  |
| C-10-15 | 35.1                  | 39.0                  | 11.64            | 10.92            | 30,000  | 4,000   |
| C-10-12 | 39.0                  | 35.1                  | 13.58            | 13.11            | 10,000  | 100,913 |
| C-10-7  | 35.1                  | 39.0                  | 13.94            | 8.98             | 100,000 | 2,386   |
| C-10-1  | 39.0                  | 35.1                  | 13.24            | 8.03             | 20,000  | 5,273   |
| C-10-11 | 35.1                  | 39.0                  | 13.58            | 12.32            | 5,273   | 4,439   |
| C-10-2  | 31.2                  | -                     | 13.24            | -                | 424,238 | -       |
| C-10-16 | 39.0                  | 31.2                  | 13.41            | 12.04            | 10,000  | 320,278 |
| C-10-6  | 31.2                  | -                     | 13.02            | -                | 220,074 | -       |
| C-10-5  | 31.2                  | 39.0                  | 13.76            | 11.27            | 320,000 | 5,440   |
| C-10-4  | 39.0                  | 31.2                  | 13.24            | 12.32            | 10,000  | 123,135 |
| C-10-19 | 31.2                  | 39.0                  | 13.24            | 11.52            | 123,135 | 3,643   |
| C-10-10 | 31.2                  | -                     | 13.58            | -                | 200,933 | -       |
| B-6-10  | 39.0                  | 31.2                  | 13.94            | 7.21             | 30,077  | 6,239   |
| B-6-14  | 31.2                  | 39.0                  | 15.14            | 13.24            | 100,000 | 30,077  |

\* $\sigma_{a1}$ ,  $\sigma_{a2}$  indicate stress amplitudes in block 1 and block 2 loading, respectively.

\*\* $E_0$  and  $E_1$  denote Young's moduli at the virgin and damaged state, respectively.

**Table 5.** Decrease of Ultimate Tensile Strength with a Uniaxial Fatigue ( $\sigma_a = 46.8$  MPa)

| Specimen Number | $n_1$ | $\sigma'_{UTS}$ (MPa) |
|-----------------|-------|-----------------------|
| B-8-6           | 1,500 | 143.4                 |
| B-8-5           | 2,000 | 141.9                 |
| B-8-8           | 3,000 | 140.3                 |
| B-8-2           | 5,000 | 127.1                 |
| B-8-3           | 7,700 | 132.5                 |
| B-8-1           | 9,900 | 118.5                 |

## 5. DISCUSSION

If a specimen has a fatigue limit, say  $\sigma_a^{fl}$ , then in a two-step loading fatigue with  $\sigma_1 = \sigma_a^{fl}$  and  $\sigma_2 > \sigma_a^{fl}$ ,  $N_1$  becomes an infinite quantity and  $n_2$  equals  $N_2$ . For this case Miner's coefficient becomes

$$M = \frac{n_1}{N_1} + \frac{n_2}{N_2} = 1$$

However if the loading sequence is reversed, there will be a continuous decrease of residual strength during the first loading. After  $n_1$  cycles the fatigue limit for this specimen is less than  $\sigma_a^{fl}$ . Because  $n_2$  and  $N_2$  are a finite and an infinite quan-

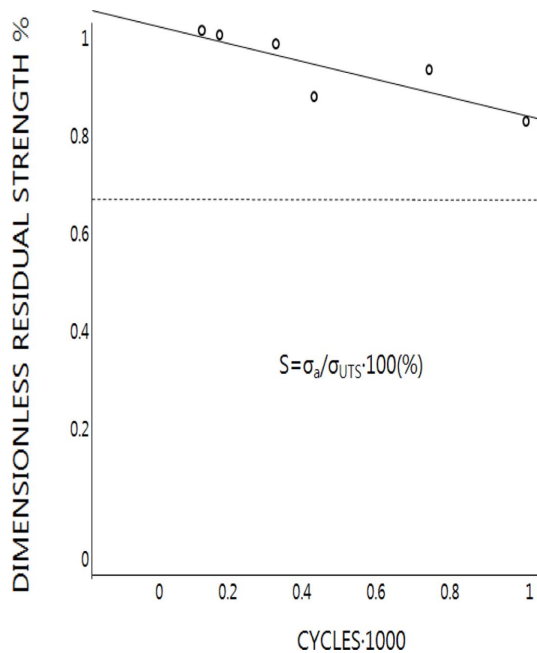


**Fig. 8.** Residual strength (made dimensionless by dividing by 145 MPa) after prior uniaxial fatigue cycling at  $R=0$ ,  $S=32\%$ . Dashed line represents the maximum stress in a cycle

tity, respectively, and  $n_1$  is less than  $N_1$ , Miner's coefficient becomes

$$M = \frac{n_1}{N_1} + \frac{n_2}{N_2} < 1$$

It is shown that Miner's coefficient is greater than one in a high-low loading sequence with the definition of failure by approach II.

## 6. CONCLUSION

- 1) A new concept of the definition of damage at failure by approach I and approach II is introduced.
- 2) Based on experimental results, the effect of mean stress on fatigue life is very small compared to the stress amplitude.
- 3) The sequence effects in two-step uniaxial fatigue for [ $\pm 45$ ]<sub>s</sub> graphite/epoxy tubular specimen shows that a high-low block loading sequence less damaging than a low-high one.

## ACKNOWLEDGEMENTS

This work was supported by a 2-year research grant from Pusan National University.

## REFERENCES

1. Stephens, R.I., Fatemi, A., Stephens, R.R., and Fuchs, O., "Metal Fatigue in Engineering", 2nd Edition, John Wiley & Sons, Inc.,

New York, 2001.

2. Krajcinovic, D. and Srinivasan, M.G., "Observations on Damage and Plasticity," Workshop on a Continuum Mechanics Approach to Damage and Life Prediction, edited by Stouffer, D.C. *et al.*, May 4-7, 1980, General Butler State Lodge, Carrollton, Kentucky, pp. 88-89.
3. Lemaitre, J., "How to Use Damage Mechanics," *Nuclear Engineering and Design*, Vol. 80, 1984, pp. 233-245.
4. Palmgren, A.Z., Die Lebensdauer von Kugellagern, *Z. ver. Deutch. Ing.* Vol. 68, 1924, pp. 339-341.
5. Miner, M.A., "Cumulative Damage in Fatigue," *Journal of Applied Mechanics*, Vol. 12, 1945, pp. A159-A164.
6. Ben-Amoz, M. and Bui-Quoc, T., "Discussion of a Reinterpretation of the Palmgren-Miner Rule for Fatigue Life Prediction," *Journal of Applied Mechanics*, Vol. 48, 1981, pp. 446-448.
7. Yang, J.N. and Jones, D.L., "Effect of Load Sequence on the Statistical Fatigue of Composites, AIAA, 18, No. 12, Dec. 1980, pp. 1525-1531.
8. Hashin, Z. and Rotem, A., "A Cumulative Damage Theory of Fatigue Failure," *Materials Science and Engineering*, Vol. 34, 1978, pp. 147-160.
9. Hashin, Z., "A Reinterpretation of the Palmgren-Miner Rule for Fatigue Life Prediction," *ASME Journal of Applied Mechanics*, Vol. 47, 1980, pp. 324-328.
10. Subramanyan, S., "A Cumulative Damage Rule Based on the Knee Point of the S-N Curve," *ASME Journal of Engineering Materials and Technology*, Vol. 98, 1976, pp. 316-321.
11. Broutman, L.J. and Sahu, S., "A New Theory to Predict Cumulative Fatigue Damage in Fiberglass Reinforced Plastics," *ASTM STP 497*, 1972, pp. 170-188.
12. Bogganoff, J.L., "A New Cumulative Damage Model, Part 1," *ASME Journal of Applied Mechanics*, Vol. 45, 1978, pp. 246-250.
13. Hashin, Z., "Statistical Cumulative Damage Theory for Fatigue Life Prediction," *ASME Journal of Applied Mechanics*, Vol. 50, 1983, pp. 571-579.
14. Yang, J.N. and Jones, D.L., "Load Sequence Effects on the Fatigue of Unnotched Composite Materials," *Fatigue of Fibrous Composite Materials*, ASTM STP 723, 1981, pp. 213-232.
15. Chou, P.C., "A Cumulative Damage Rule for Fatigue Composite Materials," *Modern Development in Composite Materials and Structure*, ed. by J. R. Vinson, ASME, 1984, pp. 343-356.
16. Bengtsson, A. and Rychlik, I., "Uncertainty in Fatigue Life Prediction of Structures Subject to Gaussian Loads," *Probabilistic Engineering Mechanics*, Vol. 24, 2009, pp.224-235.
17. Rychlik, I. and Gupta, S., "Rain-flow fatigue Damage for Transformed Gaussian Loads," *International Journal of Fatigue*, Vol. 29, 2007, pp. 406-420.
18. Bui, H.D., Dang Van, K., and de Langre, E., "A Simplified Analysis of Creep Crack Growth Using Local Approach," International Seminar on Local Approach of Fracture, Moret-sur-Loing, France, June 3-5, 1986, pp. 373-388.
19. Bui-Quoc, T., "An Engineering Approach for Cumulative Damage in Metals under Creep Loading," *Journal of Engineering Materials and Technology*, Vol. 101, 1979, pp. 337-343.
20. Paris, P.C. and Erodogan, F., "A Critical Analysis of Crack Prop-



- agation Laws," *ASME Journal of Basic Engineering*, Ser. D, 85, No. 3, 1963, pp. 528.
21. Ostergren, W.J. and Krempl, E., "A Uniaxial Damage Accumulation Law for Time-Varying Loading Including Creep-Fatigue Interaction," *ASME Journal of Pressure Vessel Technology*, Vol. 101, 1979, pp. 118-124.
  22. Niu, T.-M., "Biaxial Fatigue of Graphite/Epoxy [ $\pm 45$ ]<sub>s</sub> Tubes," Ph.D. thesis, Rensselaer Polytechnic Institute, 1983.
  23. Ayar, Tahir, "Biaxial Fatigue of Graphite/Epoxy [ $0/\pm 45$ ]<sub>s</sub> Tubes," Master's Thesis, Rensselaer Polytechnic Institute, 1984.